Electronic Supplementary Information (ESI)

Stimuli Responsive Aggregation-Induced Emission of Bis(4-((9H-fluoren-9-ylidene)methyl)phenyl)thiophene Single Crystals

Maxim S. Kazantsev, Alina A. Sonina, Igor P. Koskin, Peter S. Sherin, Tatyana V. Rybalova, Enrico Benassi and Evgeny A. Mostovich

Content

1. Characterisation

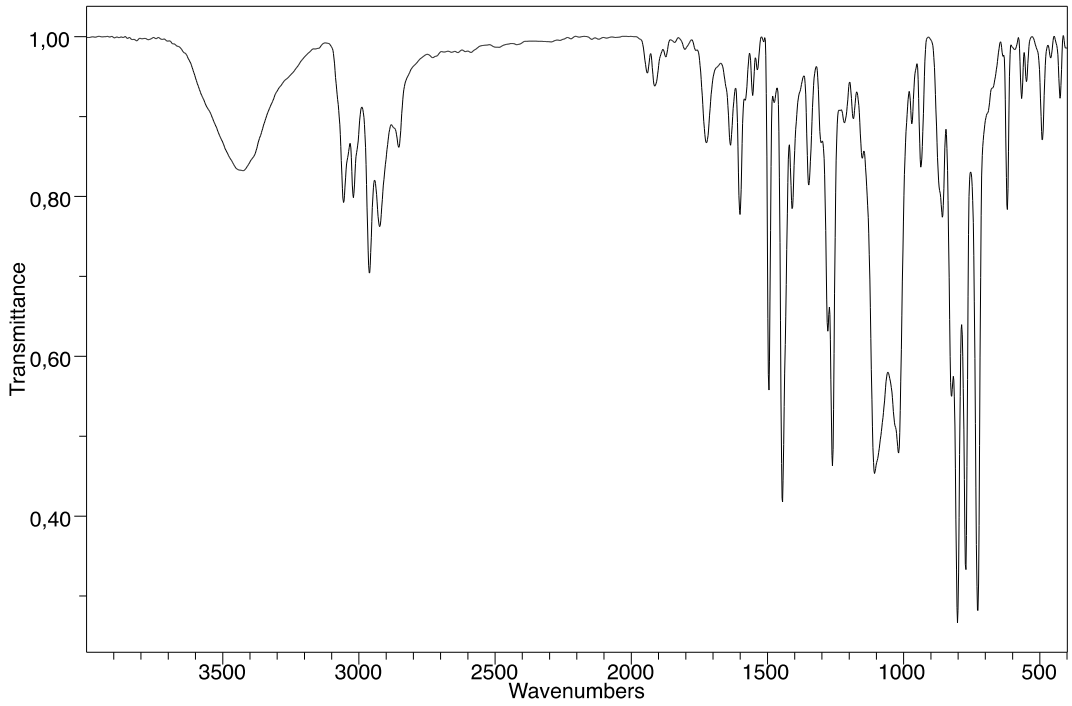

Figure S1. FT-IR spectrum of **BFMPT** recorded in KBr.

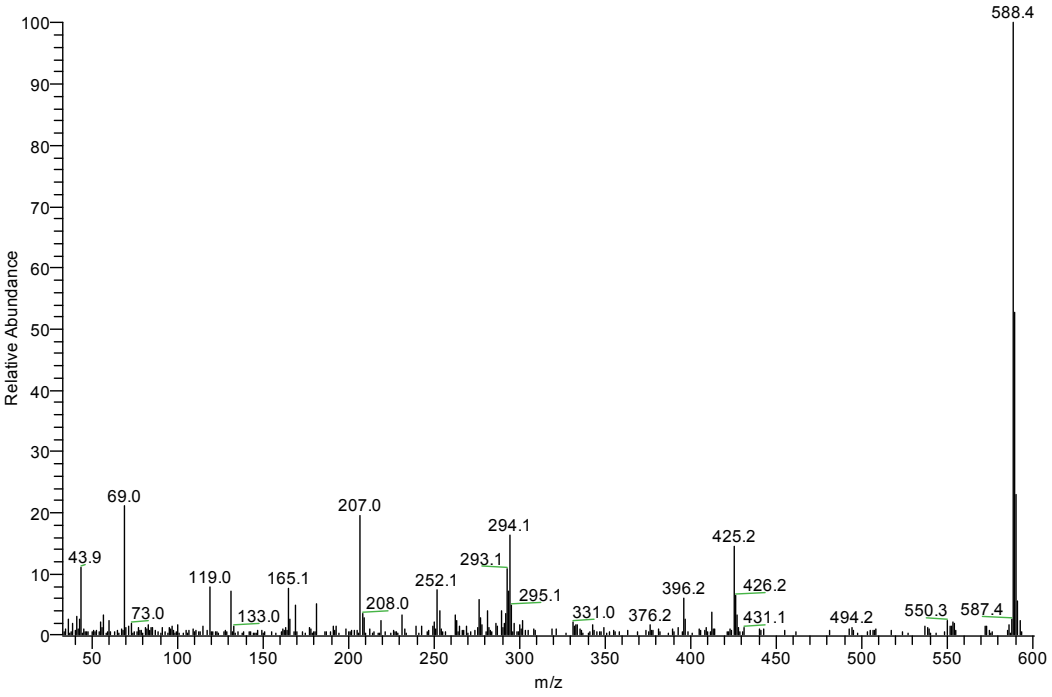

Figure S2. HR-MS spectrum of **BFMPT**.

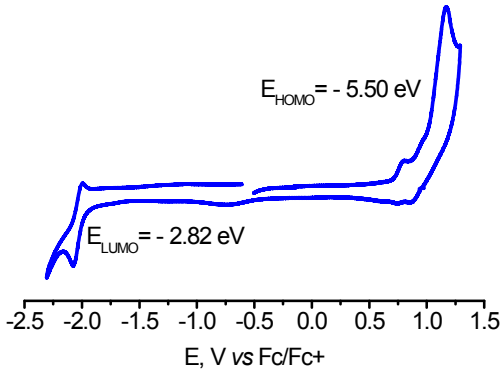

Figure S3. Cyclic voltammogramm of BFMPT in CH_2Cl_2 solution.

2. Microscopy

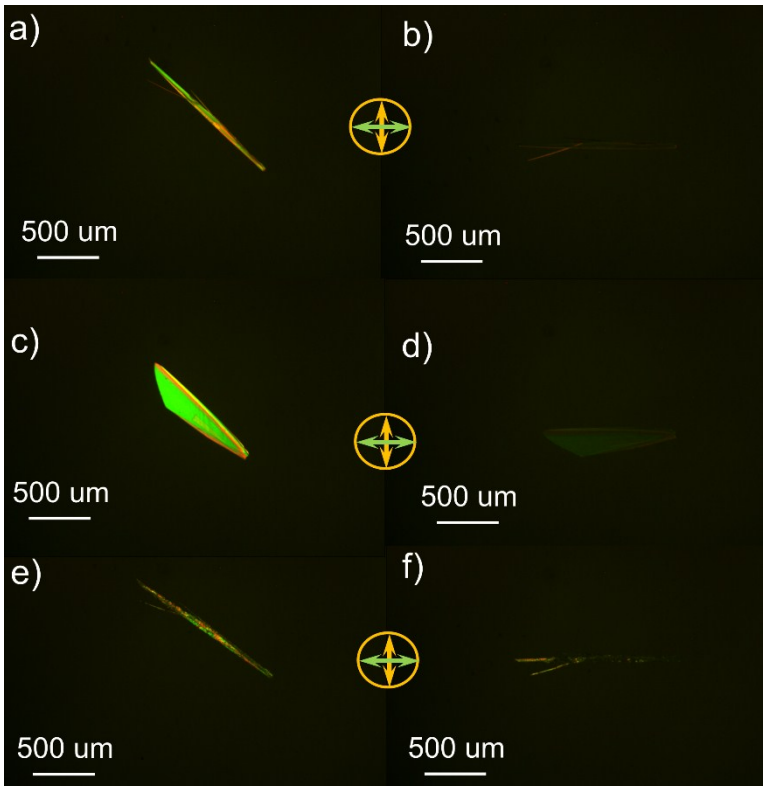

Figure S4. Optical images of the crystals in transmitted light through the crossed polarizers upon rotation of the sample holder; a, b) Form I; c, d) Form II; e, f) Form I after heating at 280 °C for 5 seconds; the arrows indicate the orientation of polarizer (orange) and analyzer (green).

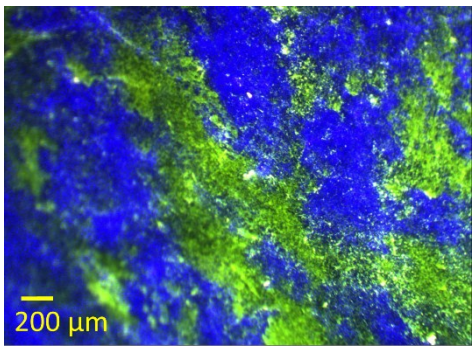

Figure S5. Optical image under blue laser irradiation (405 nm) of form I crystals after grinding in a mortar.

3. Thermal analysis

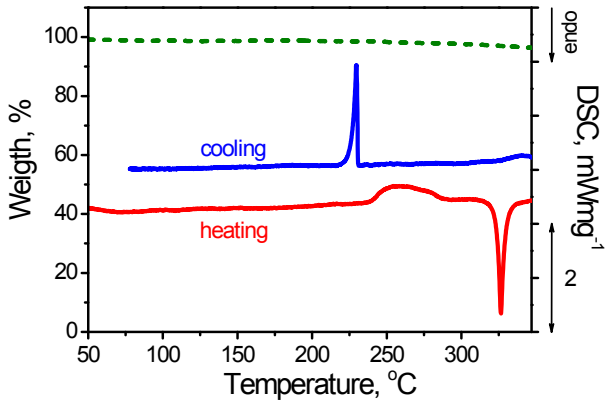

Figure S6. Thermogravimetric (olive dashed line) and differential scanning calorimetry (solid lines) analyses of the mixture of forms I and II in Ar atmosphere.

.

4. X-ray data

Table S1. Crystal data, data collection and structure refinement parameters for crystal structures of **BFMPT**.

	Form I	Form II
Chemical formula	$C_{44}H_{28}S$	
M_r	588.72	
Cryst. system, space group	Triclinic, *P*-1	Monoclinic, $P2_1/c$
a, *b*, *c* (Å)	9.7394 (3), 9.8279 (3), 16.0542 (5)	15.4125 (9), 9.8016 (5), 20.925 (1)
α, β, γ (°)	96.661 (1), 100.097 (1), 92.178 (1)	90.00, 105.660(2), 90.00
V (Å^3)	1499.98 (8)	3043.7(3)
Z	2	4
$Density_{calcd}$ (Mg.m^{-3})	1.303	1.285
F(000)	616	1232
Crystal size (mm)	0.67 × 0.18 × 0.03	1.00 × 0.50 × 0.02
μ (mm^{-1})	0.14	
T_{min}, T_{max}	0.844, 0.862	0.851, 0.862
Θ range for data collection (°)	3.046-25.10	2.937-25.027
Index ranges	-11 ≤ h ≤ 11, -11 ≤ k ≤ 11, -19 ≤ l ≤ 19	-18 ≤ h ≤ 18, -11 ≤ k ≤ 11, -24 ≤ l ≤ 24
No. of reflections measured independent observed [$I > 2\sigma(I)$]	 43942 5296 4021	 35165 5367 3983
No. of parameters	406	
R_{int}	0.039	0.048
$R[F^2 > 2\sigma(F^2)]$, $wR(F^2)$	0.036, 0.094	0.044, 0.116,
Goodness of fit, S	1.03	1.04
$\Delta\rho_{max}$, $\Delta\rho_{min}$ (e Å^{-3})	0.18, -0.19	0.22, -0.16

Table S2. The intermolecular C-H···π and π···π interactions in the crystals of BFMPT. (cycle numbering is shown in figure 2)

Form	C-H··· interaction	H···Cg* (Å)	D_{pln}*(Å)	C-H···Cg*(°)
I	C20a-H···Cg(1)	2.97	2.81	133
	C28b-H···Cg(3)	2.99	2.98	129
	C13-H···Cg(6a)	2.76	2.72	146
	C16-H···Cg(6a)	2.94	2.78	149
	C26a-H···Cg(4b)	3.00	2.91	125
	C23a-H···Cg(5b)	2.98	2.88	143
	··· interaction	Cg···Cg** (Å)	D_{pln}** (Å)	α **
	Cg(2) ··· Cg(3)	4.04	3.37/3.63	11
	Cg(4b) ··· Cg(4b)	4.00	3.51	0
II	C20a-H···Cg(1)	2.75	2.75	154
	C20b-H···Cg(1)	2.78	2.77	147
	C13-H···Cg(6a)	2.77	2.69	164
	C16-H···Cg(6a)	2.98	2.78	140

* H···Cg – distance from hydrogen atom to the center and D_{pln}- to the plane of aromatic cycle, C-H···Cg – the angle between C-H bond and the line connecting the center of aromatic cycle with H-atom.

** Cg···Cg – center to center, D_{pln} – center to plane distance and α- interplane angle for interacting cycles.

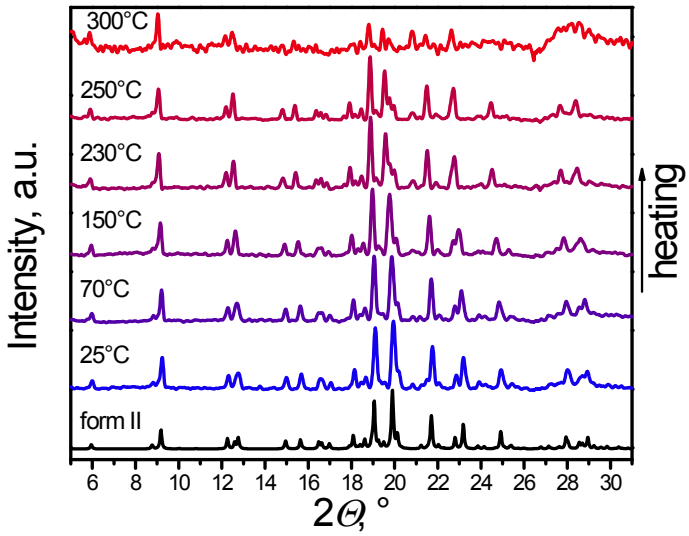

Figure S7. Variable-temperature X-ray diffraction patterns of form I after grinding in comparison with the pattern of form II (black) simulated from single crystal X-ray data.

5. Optical data

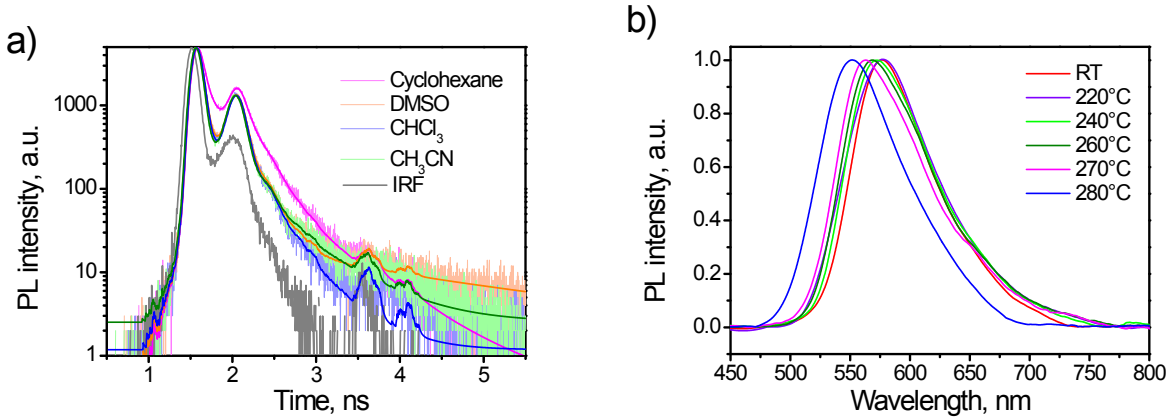

Figure S8. a) PL kinetics of BFMPT in various solvents; b) PL spectra of form I crystals after stepwise heating for 5 seconds at different temperatures: room temperature (red), 220°C (violet), 240°C (green), 260°C (olive), 270°C (magenta) and 280°C (blue).

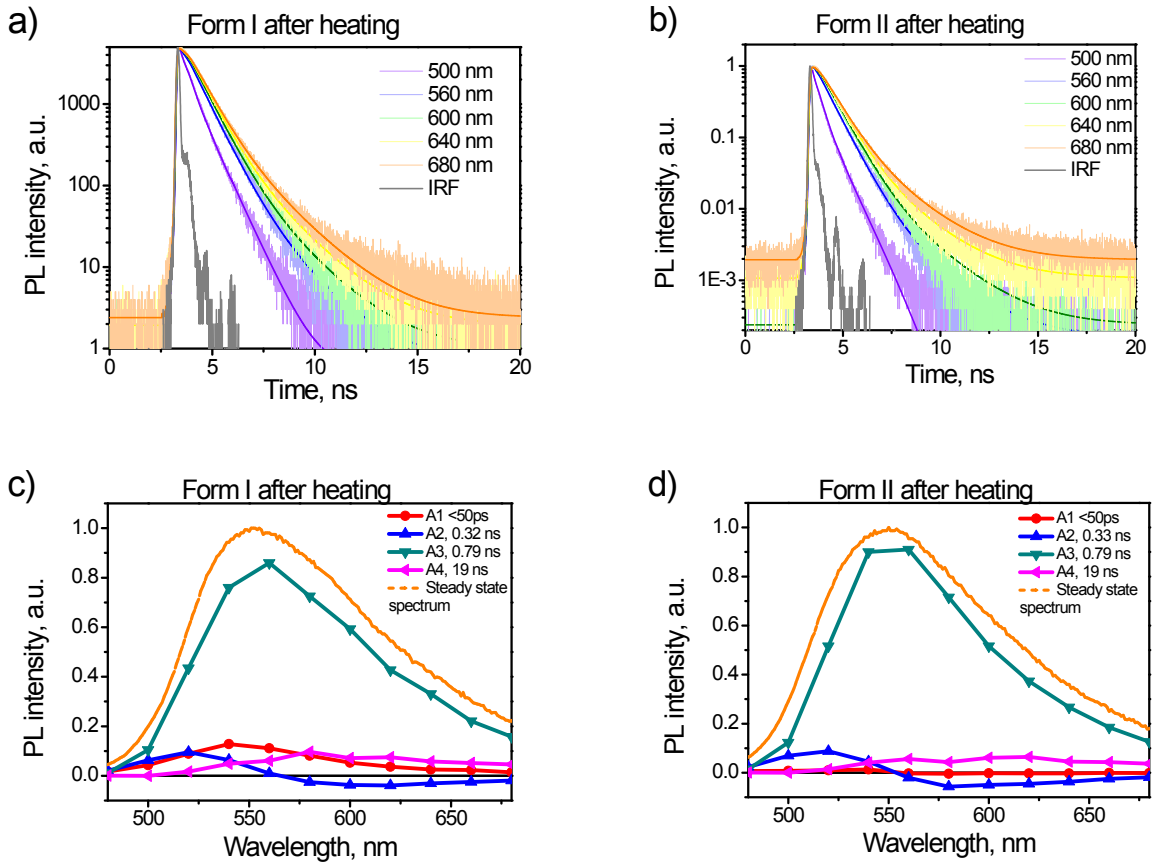

Figure S9. PL kinetics of BFMPT polymorphs after heating at 280°C for 5 seconds: PL time profiles recorded with form I after heating (a) and form II after heating (b) over the whole emission band after the excitation at 375 nm; the solid lines represent 4-exponential fits convoluted with instrument response function (IRF); decay associated spectra obtained from 4 exponential fit of fluorescence time profiles for form I after heating (c) and form II after heating (d) in comparison with steady-state spectra recorded using 375 nm laser excitation.

6. Quantum Chemical Calculations

Computational details

BFMPT ground state geometry was fully optimised both in the gas and solvated phase at Density Functional Theory (DFT), using B3LYP[1] hybrid functional coupled with triple-ζ 6-311++G**[2, 3] basis set including third generation Grimme's empirical dispersion with Becke-Johnson damping (GD3BJ).[4] This level of theory was previously shown to successfully describe geometry of thiophene/phenylene co-oligomers.[5, 6] The initial guess for the atomic position was adopted from form I and form II crystal structures. Solvent effects were accounted by mean of the SMD solvation model.[7] Solvents were chosen amongst those used in the experiments, *viz*. chloroform, dimethylsulphoxide and acetonitrile; the standard values of static dielectric constant and refraction index at room temperature were used. The absence of imaginary frequencies was checked for optimised geometry in harmonic approximation and minima were found to be "genuine". Dipole and quadrupole moment were evaluated for optimised geometry using ChElPG (Charges from Electrostatic Potentials using a Grid-based)[8] scheme of population analysis with a refined integration grid (*vide infra*).

Analysis of possible dispersive intramolecular interactions of BFMPT was performed for ground state optimised geometry in the gas phase using Non-Covalent Interaction (NCI) index(*s*) along with Reduced Density Gradient (RDG).[9] Electron densities required for RDG computations were recalculated at relaxed geometry at B3LYP/6-311++G** level of theory but with refined integration grid. Natural-Bond Orbital (NBO) analysis was also performed for electron density of relaxed single molecule evaluated at HF/6-311++G** level of theory. Statistical contribution of various intermolecular interactions in crystal structures of form I and form II was evaluated using Hirshfeld surfaces analysis based on promolecular partitioning scheme.[10]

Potential Energy Surface (PES) of BFMPT in the gas phase and in solution was explored *via* relaxed scanning around ϕ_1 and ϕ_3 dihedral angles (see Fig. 2) starting from the initial optimised geometry with nine 10-degree steps in both clockwise and counterclockwise directions, at the same level of theory adopted for optimisations.

Electronic excited states were also investigated at Time-Dependent DFT (TD-DFT) level. Tamm-Dancoff Approximation (TDA)[11] was also tested. Two different hybrid (B3LYP, PBE0)[12] and their corresponding long-range corrected (CAM-B3LYP, LC-ωPBE)[13] functionals, coupled with the double-ζ 6-31+G*basis set[14] and two triple-ζ (viz. 6-311++G** and Def2-TZVP[15]) basis sets were used. These calculations were run for the gas phase and used as a benchmarking with respect to the experimental UV-Vis absorption spectrum measured in the lowest polarity solvent (*i.e.* cyclohexane). As a result, TD-DFT CAM-B3LYP/6-311++G** level of theory was shown to give the best match and hence chosen for further investigations of excited states in solution.

UV-Vis absorption spectra were simulated in chloroform, dimethylsulphoxide, and acetonitrile solution, accounting for the first ten singlet excited states. The energy of triplet states T_n (n = 1 to 10) was also calculated in the ground state optimised geometry and alongside PES relaxed scan of around ϕ_1 and ϕ_3 dihedral angles. Solvent effects were included by means of the Polarizable Continuum Model (PCM) using the Integral Equation Formalism variant (IEFPCM).[16] PCM state specific perturbation theory both in equilibrium and non-equilibrium regimes was additionally tested for S_{1v} state. The standard Universal Force Field (UFF) radii were adopted to build up the cavity.

In order to understand the effects of surrounding molecules on the electronic excited states of BFMPT in the crystal, calculations were run at QM/MM level. TD-DFT CAM-B3LYP/6-311++G** calculations were run for single molecules (QM) in geometries adopted from form I and form II crystal structures surrounded by classical charges (MM). The values of the classical charges were the same as computed *in vacuo* at DFT B3LYP/6-311++G** level for single molecules in geometry adopted from form I and form II crystal structures, using the ChElPG scheme of population analysis. The position of the classical charges in the space was the same as of nuclei of molecules in a neighbourhood within 3.0 Å from the central (QM) molecule in the crystal; this corresponds to the first coordination sphere.

The geometry of the first singlet excited state S_1 was optimised in the gas phase at TD-DFT CAM-B3LYP/6-311++G** level of theory. S_1 PES was studied *via* relaxed scan around ϕ_1 dihedral angle from the S_{1r} initial optimised geometry with nine 10-degree steps in both clockwise and counterclockwise directions at TD-DFT B3LYP/6-311++G** level of theory in the gas phase.

In order to investigate the nature of the intermolecular interactions in the crystals, models of neighbouring dimers of BFMPT in form I and form II were built from the X-ray data and investigated at B3LYP[GD3BJ]/6-31+G* level of theory in the gas phase. The electron densities were computed and subsequently used for the RDG analysis. NBO Analysis was also carried out at HF/6-31+G* level of theory. Exciton couplings and average diffusion lengths in BFMPT dimers were calculated using the same methodology described in ref.[17] For these calculations the excited state lifetime was assumed to be 10 ps.

Integration grid for the electronic density for RDG, NBO and population analyses was set to 150 radial shells and 974 angular points. In other cases, integration grid was set as 99 radial shells and 590 angular points. The convergence criteria for Self-Consistent Field were set to 10^{-12} for root mean square (RMS) change in density matrix and 10^{-10} for maximum change in density matrix. Convergence criteria for geometry optimisations were set to 2×10^{-6} a.u. for maximum force, 1×10^{-6} a.u. for RMS force, 6×10^{-6} a.u. for maximum displacement and 4×10^{-6} a.u. for RMS displacement.

All calculations were performed using GAUSSIAN G09.D01 package.[18] The post-processing electronic density topological analysis and the calculation of the RDG and electronic density Hessian calculation were performed using MultiWFN 3.3.9 package.[19] Hirshfield surface analysis was performed using Crystal Explorer 17.[10] Visualization was performed using GaussView (v. 5.0.8).

Table S3. Coordinates of BFMPT ground state optimised geometry (gas phase). Level of theory: DFT B3LYP[GD3BJ]/6-311++G**.

S	5.25862000	7.07656400	2.75517900
C	15.18753300	11.44381100	7.38674900
H	16.10459500	11.94193100	7.67915900
C	15.18310700	10.05836000	7.19956300
H	16.09634100	9.49439800	7.34934500
C	14.01651900	9.39496500	6.81776400
H	14.03116100	8.32154700	6.66618800
C	12.84960800	10.13044700	6.63592200
C	11.49520200	9.70444500	6.21217900
C	11.17539700	8.42078300	5.93710500
H	11.93532200	7.67623300	6.16380200
C	9.94831800	7.87231300	5.35946600
C	9.29364500	8.47863200	4.27652400
H	9.70186000	9.38725600	3.85282900
C	8.15699200	7.91425900	3.72000200
H	7.69442400	8.39220700	2.86425200
C	7.61717700	6.71896200	4.22404100
C	6.41731000	6.11725600	3.65013100
C	4.23067800	5.69115500	2.45878500
C	2.98966000	5.81633500	1.70030800
C	2.31705700	7.04433500	1.58259000
H	2.70697600	7.91967200	2.08901100
C	1.14158000	7.15162900	0.85669000
H	0.63141200	8.10483100	0.80297600
C	0.57895900	6.03559400	0.21879800
C	-0.68498400	6.10926600	-0.51409400
H	-1.35732000	5.27376900	-0.33203600
C	-1.13121800	7.06178500	-1.36223500
C	-2.51281100	7.08943900	-1.89694000
C	-3.59178100	6.24176900	-1.66680100
H	-3.49729300	5.37880100	-1.01735400
C	-4.81251400	6.51561500	-2.28454500
H	-5.65797900	5.85876700	-2.11655100
C	-4.95785400	7.63107400	-3.11469500
H	-5.91519100	7.82971500	-3.58233000
C	9.62232500	13.51739700	6.47659500
H	9.20284700	14.51273700	6.56654600
C	10.98421600	13.31540100	6.69709500
H	11.62403300	14.14617600	6.97214700
C	11.50251400	12.03056200	6.57697100
C	12.85724300	11.52929300	6.82554400
C	10.67315300	10.93905600	6.21457400
C	9.30741800	11.15079400	6.02935300
H	8.64221600	10.33183600	5.79668200
C	8.79127200	12.44056200	6.15923800
H	7.73015700	12.60618400	6.01369700
C	9.43185300	6.65622500	5.83630200
H	9.92766000	6.15803800	6.66233500
C	8.28226600	6.10157600	5.29681900
H	7.88323600	5.18808700	5.72006000
C	6.00453300	4.80495900	3.69971000
H	6.57661500	4.02849300	4.18893000
C	4.77952600	4.56602700	3.03140800
H	4.30502600	3.59521200	2.98828500
C	2.41794500	4.69463700	1.07631800
H	2.91930600	3.73640500	1.13316600
C	1.23014100	4.80030000	0.37053300
H	0.80835100	3.91830200	-0.09906200
C	-2.66273600	8.21512500	-2.73545800
C	-3.88314800	8.49037700	-3.34412300
H	-4.00181200	9.35582400	-3.98611000
C	-1.37411300	8.91053200	-2.79995200
C	-0.99086000	10.02459700	-3.53875700
H	-1.70784100	10.54959800	-4.15966500
C	0.33690300	10.44677800	-3.48418400
H	0.65162100	11.31314300	-4.05437600
C	1.26879500	9.74772600	-2.71357300
H	2.30304200	10.07125300	-2.69795800
C	0.88795000	8.63432600	-1.96385000
H	1.62983900	8.10194600	-1.38637100
C	-0.44339400	8.22014200	-1.98281700
C	14.02367300	12.18951500	7.19863000
H	14.03301900	13.26403800	7.34194100

Table S4. Coordinates of BFMPT ground state optimised geometry (chloroform). Level of theory: DFT B3LYP[GD3BJ]/6-311++G** with SMD solvation model.

S	5.23030500	7.12786000	2.75521700
C	15.26681600	11.35316500	7.34801400
H	16.20356000	11.81961300	7.63689900
C	15.24261200	9.99530600	7.02481800
H	16.16095800	9.41788400	7.06597600
C	14.05602200	9.37406700	6.64478700
H	14.05874900	8.31986500	6.38412800
C	12.88619200	10.12514500	6.60157100
C	11.51269200	9.74666500	6.20848700
C	11.17962000	8.48649200	5.84927400
H	11.95714600	7.73524600	5.98435200
C	9.93671900	7.95371600	5.29796300
C	9.20097000	8.61550800	4.30673000
H	9.54761400	9.57209900	3.93115100
C	8.06229900	8.04671600	3.76227400
H	7.53974500	8.57756100	2.97193500
C	7.59902900	6.79480100	4.19124200
C	6.39966600	6.18474500	3.62710700
C	4.21624300	5.74947300	2.45446500
C	2.96890300	5.87674800	1.70770700
C	2.34351100	7.11850100	1.52513900
H	2.76989600	8.01216100	1.97127900
C	1.16608400	7.23062300	0.80593500
H	0.69476700	8.20238800	0.70516000
C	0.55215000	6.10360700	0.24511300
C	-0.72254800	6.17492300	-0.46513000
H	-1.41746100	5.37584200	-0.20830300
C	-1.16282900	7.07297600	-1.37431800
C	-2.55217100	7.08800300	-1.87731300
C	-3.64678200	6.29874100	-1.54125300
H	-3.56114900	5.49930700	-0.81144300
C	-4.87123800	6.54637700	-2.15600100
H	-5.73074700	5.93253000	-1.90521000
C	-5.00805900	7.57805900	-3.08645700
H	-5.97221900	7.75654000	-3.55234900
C	9.69593300	13.52215200	6.90732700
H	9.29001000	14.50856800	7.10912100
C	11.05983900	13.29095200	7.05496300
H	11.71998500	14.08810700	7.38337900
C	11.55787000	12.02045300	6.79193600
C	12.91481700	11.49393400	6.92693500
C	10.70734000	10.97686600	6.36098700
C	9.33966200	11.21686300	6.24498400
H	8.65396600	10.43033700	5.95515300
C	8.84406600	12.48920700	6.51721500
H	7.77881900	12.67686400	6.42579700
C	9.49483500	6.68329300	5.69779000
H	10.05661700	6.13701900	6.45022700
C	8.34237400	6.12520700	5.17490700
H	8.00995200	5.15867900	5.53798200
C	6.00159400	4.86886600	3.67078600
H	6.58143100	4.09188800	4.15477900
C	4.77778400	4.62460100	3.01267900
H	4.31560100	3.64591400	2.96371300
C	2.34677500	4.74529100	1.15838100
H	2.80469700	3.76832100	1.26948600
C	1.15483900	4.85610200	0.46481700
H	0.68938800	3.96209000	0.05979900
C	-2.69529700	8.13023400	-2.81182000
C	-3.92021000	8.37948200	-3.42050200
H	-4.03118200	9.18344000	-4.14191700
C	-1.39707300	8.78393200	-2.96534200
C	-1.00950500	9.81879100	-3.80796900
H	-1.72994900	10.29901300	-4.46311400
C	0.32269800	10.21972200	-3.81104200
H	0.64278300	11.02635500	-4.46325100
C	1.25326600	9.57981400	-2.99282100
H	2.29400700	9.88731100	-3.01928300
C	0.86748100	8.54809600	-2.14110300
H	1.61264000	8.06099300	-1.52435700
C	-0.46851700	8.15427400	-2.10584700
C	14.10233100	12.11390400	7.29889900
H	14.12656800	13.17091600	7.54578300

Table S5. Coordinates of BFMPT ground state optimised geometry (acetonitrile). Level of theory: DFT B3LYP[GD3BJ]/6-311++G** with SMD solvation model.

S	5.20997500	7.16290800	2.75572900
C	15.32832000	11.29466300	7.30798500
H	16.27667600	11.74231100	7.58888700
C	15.27966900	9.94406100	6.95474100
H	16.19084500	9.35392500	6.96548700
C	14.07802700	9.34545200	6.58398500
H	14.06224800	8.29676900	6.30255800
C	12.91670100	10.11249500	6.58036300
C	11.52962500	9.76055700	6.20861100
C	11.18024600	8.51239400	5.81929500
H	11.95725700	7.75472900	5.91568300
C	9.92739400	7.99102800	5.28346500
C	9.13116200	8.69176000	4.36802000
H	9.43293700	9.67912000	4.03649300
C	7.98488600	8.12473900	3.83767300
H	7.41326900	8.69441600	3.11061400
C	7.57454900	6.83400500	4.20299100
C	6.36880800	6.22609800	3.65047000
C	4.18251200	5.78812800	2.48314100
C	2.93952400	5.91043100	1.72830600
C	2.32736300	7.15398800	1.51320400
H	2.75915400	8.05522100	1.93864100
C	1.15458200	7.25996400	0.78471800
H	0.69464300	8.23435600	0.65982500
C	0.53320700	6.12500600	0.24796200
C	-0.73617600	6.18342700	-0.47201900
H	-1.42668600	5.38158200	-0.21204100
C	-1.17725000	7.06589200	-1.39693200
C	-2.56273500	7.05408000	-1.91143100
C	-3.64874800	6.25274100	-1.57317300
H	-3.55671700	5.46393800	-0.83250800
C	-4.87156200	6.47524500	-2.20183700
H	-5.72444300	5.85261100	-1.94970800
C	-5.01549300	7.49208200	-3.14871000
H	-5.97846400	7.65018600	-3.62449600
C	9.78053000	13.54131000	7.05278400
H	9.39338900	14.52757900	7.28955900
C	11.14493600	13.28860900	7.15862200
H	11.82633100	14.06695700	7.48888100
C	11.61749000	12.01803100	6.85068300
C	12.97023600	11.47269000	6.93843300
C	10.74300800	10.99525400	6.41535300
C	9.37572400	11.25710100	6.34147400
H	8.67026300	10.48926500	6.04953500
C	8.90482300	12.52880300	6.65940100
H	7.84010500	12.73222600	6.60010900
C	9.53790600	6.68366400	5.61700100
H	10.15114900	6.10549800	6.30235300
C	8.38015000	6.12420300	5.10783100
H	8.09967600	5.12252500	5.41534800
C	5.95710600	4.91463400	3.71974800
H	6.52389200	4.14182300	4.22492700
C	4.73245100	4.66862100	3.06426900
H	4.26171800	3.69312700	3.03366400
C	2.30894900	4.77074900	1.20473900
H	2.75429200	3.79167800	1.34510200
C	1.12172700	4.87652200	0.50212200
H	0.64714400	3.97746000	0.11962300
C	-2.71283600	8.07968800	-2.86354700
C	-3.93606400	8.30415400	-3.48637900
H	-4.05015300	9.09614800	-4.22053700
C	-1.42205700	8.74730700	-3.01835100
C	-1.04349300	9.77278900	-3.87716100
H	-1.76701900	10.22980400	-4.54553000
C	0.28336000	10.19263000	-3.87716700
H	0.59746200	10.99212700	-4.54107000
C	1.21638700	9.58102500	-3.03917800
H	2.25251000	9.90419000	-3.06184700
C	0.83896000	8.55886700	-2.17152000
H	1.58686200	8.09671200	-1.53914800
C	-0.49163200	8.14479700	-2.14046000
C	14.17255800	12.07081800	7.30053700
H	14.21215500	13.12140500	7.57220500

Table S6. Coordinates of BFMPT ground state optimised geometry (dimethylsulphoxide). Level of theory: DFT B3LYP[GD3BJ]/6-311++G** with SMD solvation model.

S	5.29445300	7.12455200	2.69196700
C	15.24608700	11.28141100	7.54824200
H	16.17763000	11.73147000	7.87735000
C	15.19689200	9.91091900	7.28375800
H	16.09090200	9.30815100	7.41041000
C	14.01664900	9.30775200	6.85628200
H	14.00017800	8.24217000	6.64753600
C	12.87695800	10.09163200	6.70511700
C	11.51622000	9.73631400	6.25019600
C	11.17001000	8.47055400	5.92043100
H	11.91939900	7.70711800	6.12643700
C	9.94695000	7.94076500	5.32679800
C	9.24413500	8.59398700	4.30581300
H	9.60483800	9.54309000	3.92495700
C	8.11785600	8.02443200	3.73698800
H	7.62019400	8.55095700	2.92786300
C	7.63586000	6.78023600	4.16882500
C	6.44155900	6.17606400	3.58868700
C	4.26531900	5.75502100	2.39915200
C	3.02304100	5.88825100	1.64551900
C	2.41824600	7.13651000	1.43673500
H	2.85959600	8.03423400	1.85984200
C	1.23867200	7.25203500	0.72134500
H	0.78304500	8.22975600	0.60871300
C	0.60219900	6.12237300	0.19061400
C	-0.67868800	6.18324000	-0.50540800
H	-1.34729500	5.35870000	-0.25985000
C	-1.16237100	7.08650300	-1.38877100
C	-2.56154900	7.05686100	-1.86333100
C	-3.61639700	6.21622600	-1.52222200
H	-3.48305000	5.40535500	-0.81222700
C	-4.86219000	6.42794100	-2.10745900
H	-5.69136400	5.77490500	-1.85322100
C	-5.05967500	7.47279500	-3.01304000
H	-6.04029700	7.62251600	-3.45426500
C	9.78680000	13.59307200	6.69673800
H	9.40335500	14.59935100	6.83470500
C	11.13385500	13.32753600	6.92292700
H	11.80414500	14.11680400	7.24997300
C	11.60190400	12.03172500	6.73914200
C	12.93132500	11.47255900	6.97182300
C	10.74182400	10.99466800	6.30935900
C	9.38947100	11.27140600	6.11534200
H	8.69164600	10.49623400	5.82418400
C	8.92229600	12.56902600	6.30933000
H	7.86921300	12.78356000	6.15593700
C	9.49123600	6.67364300	5.72404100
H	10.03288400	6.13137000	6.49382500
C	8.35142200	6.11399100	5.17568600
H	8.00827500	5.15025400	5.53652600
C	6.02676500	4.86549000	3.64387000
H	6.58923500	4.08766400	4.14686900
C	4.80716700	4.62901400	2.97521300
H	4.33428200	3.65503800	2.93122800
C	2.37988600	4.75418400	1.12537600
H	2.81845400	3.77144000	1.26124300
C	1.18698400	4.86975000	0.43482500
H	0.70140200	3.97438000	0.05747400
C	-2.76484300	8.10927800	-2.77531400
C	-4.01168300	8.32396600	-3.35280300
H	-4.16787400	9.13774100	-4.05467200
C	-1.49608000	8.81377400	-2.94412900
C	-1.16868000	9.87620300	-3.77838900
H	-1.92301300	10.33716200	-4.40898800
C	0.14693000	10.32885600	-3.80359400
H	0.42118400	11.15788200	-4.44869400
C	1.11932500	9.71298200	-3.01528500
H	2.14628900	10.06228500	-3.05808200
C	0.79339400	8.65368400	-2.17182200
H	1.57208400	8.18992200	-1.57905000
C	-0.52542300	8.20601600	-2.11440100
C	14.11251600	12.07429000	7.39221100
H	14.15333500	13.14010200	7.59599300

Table S7. Values of the ground, S_{1v} (Franck-Condon region) and S_{1r} states electric dipole moment (μ; in Debye) and the diagonal components of the quadrupole moment ($\Theta_{\alpha\alpha}$, $\alpha = x, y, z$ referring to the standard orientation of the molecule; in Debye · Ångstrøm) evaluated for BFMPT molecule, optimised in the gas phase and in the various solvents (chloroform, acetonitrile, dimethylsulphoxide)

	μ /D	Θ_{xx} / (D·Å)	Θ_{yy} / (D·Å)	Θ_{zz} / (D·Å)
Gas phase (S_0)	1.4535	-264.783	-265.734	280.922
Chloroform (S_0)	2.3345	-282.675	-271.186	-241.798
Acetonitrile (S_0)	2.6954	-284.693	-272.282	-240.158
Dimethylsulphoxide (S_0)	2.8420	-284.166	-263.532	-249.155
Gas phase (S_{1v})	3.1284	-279.124	-262.114	-234.572
Chloroform (S_{1v})	3.3161	-301.919	-278.008	-248.706
Acetonitrile (S_{1v})	3.7800	-310.140	-284.671	-249.264
Dimethylsulphoxide (S_{1v})	3.8024	-303.082	-280.768	-247.762
Gas phase (S_{1r})	1.8810	-285.624	-270.204	-249.298

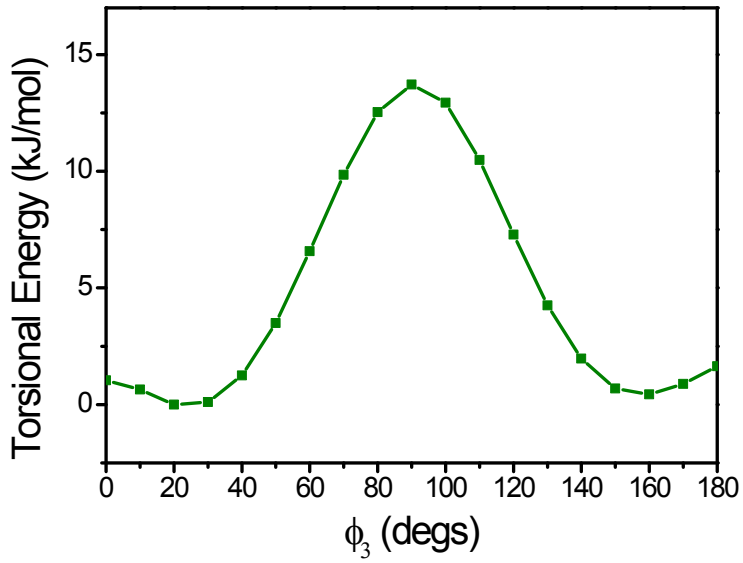

Figure S10. Ground state potential energy of BFMPT evaluated as a function of ϕ_3 dihedral angle. Level of theory: DFT B3LYP[GD3BJ]/6-311++G**.

Table S8. Deviation of TD (TDA) calculated transition energy (in eV). using different combinations of functionals and basis sets. for the brightest absorption band with respect to the experimental UV-Vis absorption data for BFMPT. Geometry optimised at DFT B3LYP[GD3BJ]/6-311++G** level of theory.

	TD			
Basis set	B3LYP	CAM-B3LYP	PBE0	LC-ωPBE
6-31+G*	-0.41331	0.10519	-0.29381	0.46029
6-311++G**	-0.43081	0.09689	-0.29151	0.43339
Def2-TZVP	-0.43971	0.08459	-0.30921	0.42789
	TDA			
	B3LYP	CAM-B3LYP	PBE0	LC-ωPBE
6-31+G*	-0.34911	0.19899	-0.24381	0.58139
6-311++G**	-0.36651	0.17749	-0.22561	0.55619
Def2-TZVP	-0.36121	0.17959	-0.24081	0.54919

Table S9. Ground to S_{1v} state excitation energy (in eV) computed in (a) linear response (LR) nonequilibrium (neq) solvation regime. (b) state-specific (SS) equilibrium (eq) solvation regime. and (c) state specific nonequilibrium solvation regime. Geometry optimised at DFT B3LYP[GD3BJ]/6-311++G** level of theory with SMD solvent simulation. Excited states computed at TD CAM-B3LYP/6-311++G** level of theory.

	LR/neq	SS/eq	SS/neq
Chloroform	3.1105	3.0462	3.0863
Acetonitrile	3.0897	2.9721	3.0214
Dimethylsulphoxide	3.0125	3.0211	3.0501

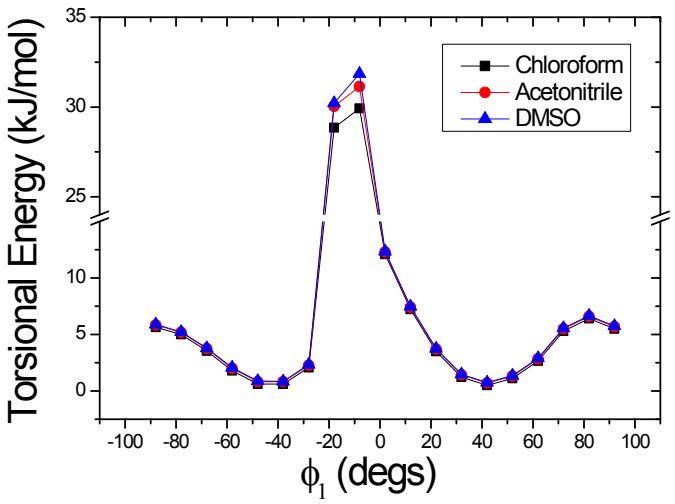

Figure S11. Ground state potential energy of BFMPT evaluated as a function of ϕ_1 dihedral angle evaluated at a set of different solvents (chloroform. acetonitrile. dimethylsulphoxide). Level of theory: DFT B3LYP[GD3BJ]/6-311++G** with SMD solvation model.

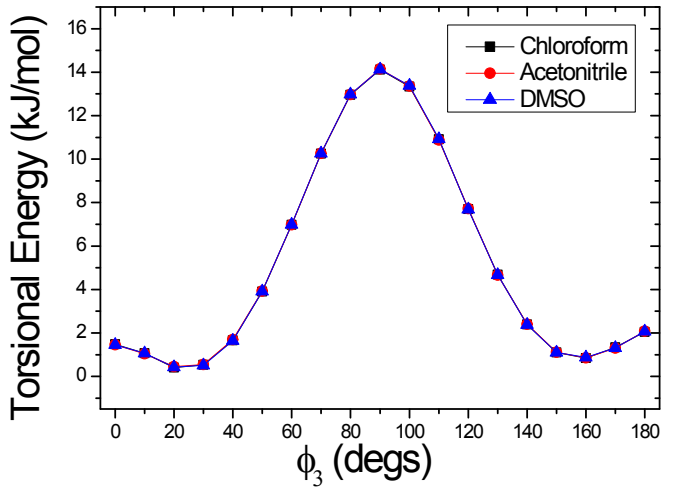

Figure S12. Ground state potential energy surface of BFMPT evaluated as a function of ϕ_3 dihedral angle evaluated at a set of different solvents (chloroform. acetonitrile. dimethylsulphoxide). Level of theory: DFT B3LYP[GD3BJ]/6-311++G** with SMD solvation model.

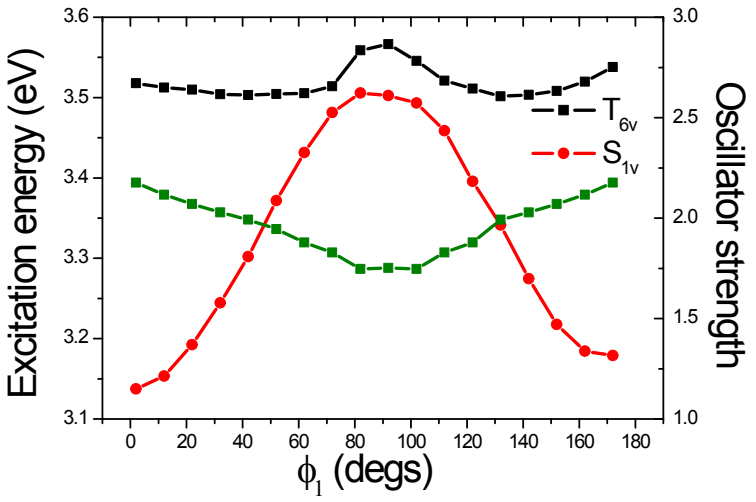

Figure S13. Relative energy (with respect to energy of ground state) of the vertically excited states T_{6v} (black squares) and S_{1v} (red circles) evaluated along φ_1 PES scan of BFMPT. The oscillator strength for the transition from ground to S_{1v} state is also depicted (green squares).

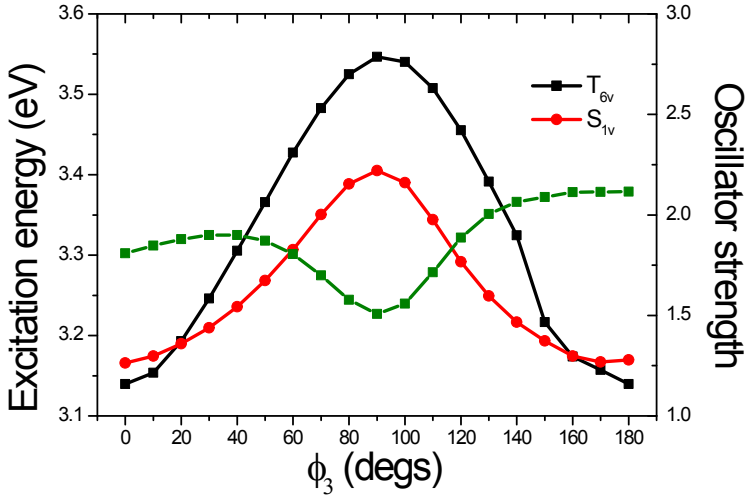

Figure S14. Relative energy (with respect to energy of ground state) of T_{6v} (red circles) and S_{1v} vertical excited levels (black squares) evaluated along φ_3 PES scan of BFMPT. Green line represents the oscillator strength of S_{1v} state.

Table S10. Inductive (*i*) and orientational (*o*) contributions to the solvatochromic shift (in eV), due to the change of the electric dipole moment (**μ**) and quadrupole moment (**Θ**). Lippert-Mataga, McRae and Suppan models were employed using quantum mechanical values of dipole and quadrupole moments (for the GS and the ES).

	Δ*E*(μ)		**Δ*E*(Θ)**	
	i	*o*	*i*	*o*
Chloroform	9.71E-05	1.80E-03	7.06E-03	4.04E-02
DMSO	6.49E-05	4.55E-03	4.15E-03	8.98E-02
Acetonitrile	6.02E-04	4.99E-03	3.22E-02	8.26E-02

Table S11. Coordinates of BFMPT S_1 state optimised geometry (gas phase). Fluorescence energy: 2.2358 eV.

S	5.26427300	7.20376300	2.62697500
C	15.26100700	11.42706500	7.25066400
H	16.19930800	11.89929000	7.51605000
C	15.25505700	10.10626000	6.80639400
H	16.18895800	9.56226100	6.73089100
C	14.06492600	9.48023000	6.45438100
H	14.08088200	8.45591700	6.10085100
C	12.87455700	10.18680300	6.56276300
C	11.48592600	9.79098900	6.23558100
C	11.17431600	8.56525100	5.76431600
H	11.98471100	7.84042500	5.77306500
C	9.93022100	8.03363100	5.22850900
C	9.04924400	8.78504900	4.43693000
H	9.28397800	9.81661100	4.21054800
C	7.91049300	8.22330100	3.90495000
H	7.26736300	8.83845000	3.28694400
C	7.58003500	6.87263800	4.13598400
C	6.38482700	6.28488500	3.59704400
C	4.19518700	5.82762500	2.41783200
C	3.00091800	5.91209900	1.67183300
C	2.57869600	7.12646700	1.05707500
H	3.16541600	8.02626000	1.20013300
C	1.44282500	7.19781000	0.31034200
H	1.13866800	8.14971900	-0.10088700
C	0.60807900	6.05251700	0.10757900
C	-0.58765600	6.07006200	-0.62305400
H	-1.25263100	5.23338300	-0.41968600
C	-1.08516400	7.01143900	-1.53093800
C	-2.50407100	7.16077300	-1.80832300
C	-3.61123900	6.50682900	-1.26510000
H	-3.49084600	5.72850000	-0.52047000
C	-4.88273500	6.86850800	-1.68900700
H	-5.74852800	6.36228400	-1.27880100
C	-5.06048000	7.88180800	-2.63206100
H	-6.06174800	8.15283300	-2.94504900
C	9.61011600	13.39848100	7.46289500
H	9.19204300	14.34102200	7.79561700
C	10.98744800	13.21308100	7.46314100
H	11.64560100	14.00213600	7.80792800
C	11.50073400	11.99912100	7.03472200
C	12.88505700	11.51661600	7.01053100
C	10.65380200	10.96724900	6.58016700
C	9.27581400	11.15494600	6.61840300
H	8.59436600	10.36946300	6.32556300
C	8.76367600	12.37105000	7.05661800
H	7.69051500	12.51718900	7.08435700
C	9.62862400	6.67383500	5.41886300
H	10.30945700	6.05847600	5.99616500
C	8.48348900	6.11066100	4.90617800
H	8.28547700	5.06429500	5.09706800
C	5.92807400	4.97410500	3.73504500
H	6.46319900	4.22284800	4.29759600
C	4.73081700	4.71752400	3.09060000
H	4.24987400	3.75051200	3.10344600
C	2.14288900	4.77869200	1.51733100
H	2.40434900	3.84161900	1.99038200
C	0.99931000	4.85368700	0.78658400
H	0.36837000	3.97750600	0.68817900
C	-2.69135600	8.18845000	-2.76297200
C	-3.96321900	8.54983900	-3.17194900
H	-4.11172200	9.33879600	-3.90059400
C	-1.36909000	8.67429300	-3.14997900
C	-0.98722400	9.61163400	-4.09192300
H	-1.72955000	10.17016500	-4.65081300
C	0.37009400	9.81667200	-4.33364200
H	0.68181300	10.54675700	-5.07100500
C	1.32831800	9.06569500	-3.65443000
H	2.37869600	9.20952900	-3.87844500
C	0.95615100	8.12484300	-2.70351200
H	1.71710600	7.53102300	-2.21556800
C	-0.39987200	7.94369200	-2.40957500
C	14.07376700	12.14295200	7.35394900
H	14.08351900	13.17091500	7.69722600

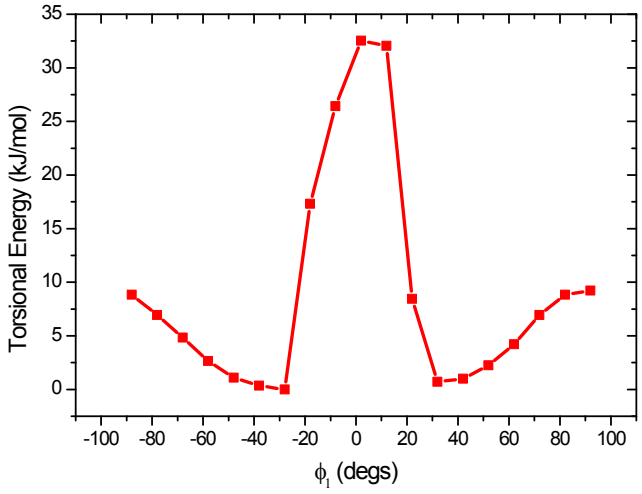

Figure S15. Relaxed scan of potential energy of S_{1r} state as a function of ϕ_1 dihedral angle. Level of theory: DFT B3LYP[GD3BJ]/6-311++G**.

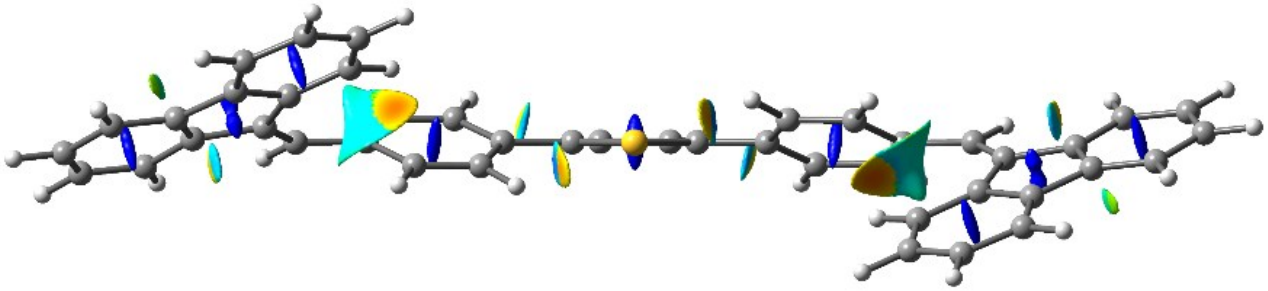

Figure S16. Plot of the RDG isosurfaces (s = 0.5 a.u. and a red-to-blue colour scale from -0.015 a.u. $\leq$ sign(λ_2) $\rho(\mathbf{r}) \leq$ +0.015 a.u.) calculated for BFMPT optimised geometry. Blue colour stands for repulsion. yellow/orange for (weak) attraction.

Table S12. Statistical contribution of various intermolecular contacts in form I and form II X-ray structures based on Hirshfeld surface analysis.

	Form I	Form II
C…C	5.1	4.2
H…H	45.2	46.0
S…S	0.0	0.0
C…H	45.8	46.3
C…S	0.4	0.0
H…S	3.5	3.5

7. References

1. A. D. Becke, *J. Chem. Phys*, 1993, **98**, 5648–5652.
2. A. D. McLean and G. S. Chandler, *J. Chem. Phys*, 1980, **72**, 5639–5648.
3. R. Krishnan, J. S. Binkley, R. Seeger and J. A. Pople, *J. Chem. Phys*, 1980, **72**, 650–654.
4. S. Grimme, S. Ehrlich and L. Goerigk, *J. Comput. Chem.*, 2011, **32**, 1456–1465.
5. I. P. Koskin, E. A. Mostovich, E. Benassi and M. S. Kazantsev, *J. Phys. Chem. C*, 2017, **121**, 23359–23369.
6. I. P. Koskin, E. A. Mostovich, E. Benassi and M. S. Kazantsev, *Chem. Commun.*, 2018, **54**, 7235-7238
7. A. V. Marenich, C. J. Cramer and D. G. Truhlar, *J. Phys. Chem. B*, 2009, **113**, 6378-6396.
8. C. M. Breneman and K. B. Wiberg, *J. Comp. Chem.*, 1990, **11**, 361-373.
9. E. R. Johnson, S. Keinan, P. Mori-Sánchez, J. Contreras-García, A. J. Cohen and W. Yang, *J. Am. Chem. Soc.*, 2010, **132**, 6498–6506.
10. M. J. Turner, J. J. McKinnon, S. K. Wolff, D. J. Grimwood, P. R. Spackman, D. Jayatilaka and M. A. Spackman, *Crystal Explorer 17*, 2017.
11. F. Trani, G. Scalmani, G. S. Zheng, I. Carnimeo, M. J. Frisch and V. Barone, *J. Chem. Theory Comput.*, 2011, **7**, 3304-3313.
12. J. P. Perdew, M. Ernzerhof and K. Burke, *J. Chem. Phys*, 1996, **105**, 9982–9985.
13. T. Yanai, D. P. Tew and N. C. Handy, *Chem. Phys. Lett.*, 2004, **393**, 51–57.
14. R. Ditchfield, W. J. Henre and J. A. Pople, *J. Chem. Phys*, 1971, **54**, 724–728.
15. F. Weigend and R. Ahlrichs, *Phys. Chem. Chem. Phys.*, 2005, **7**, 3297-3305.
16. G. Scalmani and M. J. Frisch, *J. Chem. Phys.*, 2010, **132**, 114110.
17. E. Benassi and S. Corni, *J. Phys. Chem. C.*, 2013, **117**, 25026-25041.
18. M. J. Frisch, G. W. Trucks, H. B. Schlegel, G. E. Scuseria, M. A. Robb, J. R. Cheeseman, G. Scalmani, V. Barone, G. A. Petersson, H. Nakatsuji, X. L. Caricato, M., A. Marenich, J. Bloino, B. G. Janesko, R. Gomperts, B. Mennucci, H. P. Hratchian, J. V. Ortiz, A. F. Izmaylov, J. L. Sonnenberg, D. Williams-Young, F. Ding, F. Lipparini, F. Egidi, J. Goings, B. Peng, A. Petrone, T. Henderson, D. Ranasinghe, V. G. Zakrzewski, J. Gao, N. Rega, G. Zheng, W. Liang, M. Hada, M. Ehara, K. Toyota, R. Fukuda, J. Hasegawa, M. Ishida, T. Nakajima, Y. Honda, O. Kitao, H. Nakai, T. Vreven, K. Throssell, J. A. Montgomery, J. Peralta, J. E., F. Ogliaro, M. Bearpark, J. J. Heyd, E. Brothers, K. N. Kudin, V. N. Staroverov, T. Keith, R. Kobayashi, J. Normand, K. Raghavachari, A. Rendell, J. C. Burant, S. S. Iyengar, J. Tomasi, M. Cossi, J. M. Millam, M. Klene, C. Adamo, R. Cammi, J. W. Ochterski, R. L. Martin, K. Morokuma, O. Farkas, J. B. Foresman and F. D. J., *Gaussian 09, Revision A.02*, 2016.
19. T. Lu and F. Chen, *J. Comput. Chem.*, 2012, **33**, 580–592.